Lithium−Benzene Sandwich Compounds: A Quantum Chemical Study

James M. Vollmer,*,† Anil K. Kandalam,‡,§ and Larry A. Curtiss*,†,‡

Chemistry and Materials Science Divisions, Argonne National Laboratory, Argonne, Illinois 60439

Received: March 27, 2002; In Final Form: July 30, 2002

The structures and dissociation energies of $Li_n{\cdot}(C_6H_6)_{n+1}$ sandwich complexes ($n = 1-6$) have been investigated using quantum chemical techniques. At the G3(MP2) level of theory, the $Li{\cdot}(C_6H_6)_2$ complex exhibits a Jahn−Teller distortion, forming a D_{2h} charge-separated species $[C_6H_6{}^{-1/2}-Li-C_6H_6{}^{-1/2}]$ with a surprisingly large dissociation energy of 0.85 eV, and a short benzene−benzene distance of 3.54 Å. Comparisons are made with the $Li{\cdot}C_6H_6$, $Li^+{\cdot}C_6H_6$, and $Li^+{\cdot}(C_6H_6)_2$ complexes. The larger ($n > 1$) complexes were studied at the B3LYP/6-31G(d) level and were also found to have large dissociation energies, ca. 0.85 eV per Li atom, and short benzene−benzene distances (3.70 Å).

1. Introduction

There is considerable interest in the intercalation of Li^+ into graphite, due to the widespread use of graphite/carbon anodes in lithium-ion cells. To gain a fundamental understanding of Li^+−intercalated graphite, it is necessary to understand the interactions between the lithium and π-electrons of the aromatic carbon. The $Li^+{\cdot}C_6H_6$ complex is the smallest model system that can be used to examine these interactions, and has been the topic of several gas-phase experimental[1−3] and computational studies.[3−8] The first experimental work[1] on this system used ion cyclotron resonance techniques to arrive at a Li^+ affinity (ΔH°_{298}) for C_6H_6, which Amicangelo and Armentrout converted to a 0 K value of 1.58 ± 0.08 eV.[3] Amicangelo and Armentrout[3] determined a lithium affinity at 0 K for C_6H_6 of 1.67 ± 0.14 eV, for $Li^+{\cdot}C_6H_6$, using threshold collision-induced dissociation methods. A wide range of computational methods have been used to predict lithium affinities of C_6H_6, yielding values ranging from 1.43 to 1.90 eV.[3,5,6,8] For intercalation processes, the Li^+ interacts with two sheets of graphite/ polyaromatic carbon, so $Li^+{\cdot}(C_6H_6)_2$ is perhaps a more representative model system. In their study, Amicangelo and Armentrout[3] also determined experimental and theoretical dissociation energies $[Li^+{\cdot}(C_6H_6)_2 \rightarrow Li^+ + 2C_6H_6]$ for this system at 0 K. Their experimental dissociation energy for the complex was 2.75 ± 0.21 eV. At the MP2(full)/6-311+G(2d,-2p)//MP2(full)/6-311+G* level of theory, with basis set superposition error (BSSE) corrections and thermal corrections, they found a dissociation energy of 2.57 eV.

Because the Li^+ presumably pairs with an electron once it is intercalated, the neutral analogues of these complexes are also of interest. We have found only one reference to the neutral $Li{\cdot}C_6H_6$ complex.[9] It reports HF/6-31G(d) and MP2/6-31G optimized distances between the Li atom and benzene ring of 2.511 and 2.600 Å, respectively. We have found no studies on the $Li{\cdot}(C_6H_6)_2$ complex; however, numerous studies have been performed on transition metal, lanthanide, and actinide metal, $M_n{\cdot}(C_6H_6)_{n+1}$ sandwich complexes.[10−16]

---

* Corresponding authors. James M. Vollmer (e-mail: james.vollmer@ anl.gov) and Larry A. Curtiss (e-mail: curtiss@anl.gov).
† Chemistry Division.
‡ Materials Science Division.
§ Thesis Parts Graduate Student Participant from Michigan Tech University.

TABLE 1: Optimized MP2(FC)/6-31G(d) Geometries of the $Li{\cdot}C_6H_6$ and $Li^+{\cdot}C_6H_6$ Complexes[a]

parameter	$Li{\cdot}C_6H_6$	$Li^+{\cdot}C_6H_6$
r(CC)	1.401	1.407
r(CH)	1.087	1.087
r(LiX)[a]	2.252	1.921
point group	C_{6v}	C_{6v}

[a] X refers to the center of the benzene ring. Bond distances in angstroms.

In this paper we report a quantum chemical study of the geometries, dissociation energies, and bonding of the $Li{\cdot}(C_6H_6)_2$ complexes. We have also applied these techniques to the $Li{\cdot}C_6H_6$, $Li^+{\cdot}C_6H_6$, and $Li^+{\cdot}(C_6H_6)_2$ complexes for comparison to the $Li{\cdot}(C_6H_6)_2$ complex. Due to the strong binding found for $Li{\cdot}(C_6H_6)_2$, we also investigated the geometries and dissociation energies for larger $Li_n(C_6H_6)_{n+1}$ sandwich complexes ($n = 2-6$).

2. Theoretical Methods

Geometry optimizations for the $Li{\cdot}C_6H_6$ and $Li{\cdot}(C_6H_6)_2$ complexes were performed at the HF/6-31G(d),[17] B3LYP/6-31G(d),[18,19] and MP2(FC)/6-31G(d)[17] levels of theory. Single-point energies were obtained at the G3(MP2)[20] level of theory, as well as at the intermediate levels required for a G3(MP2) calculation: MP2/G3MP2Large[20] and QCISD(T)/6-31G(d). The G3MP2Large basis set is the same as 6-311++G(2df,2p) for first row atoms.[20] Frequency calculations were performed using the HF/6-31G(d), MP2(FC)/6-31G(d), and B3LYP/6-31G(d) methods to verify that the optimized structures were true minima. Zero-point energy contributions for G3(MP2) theory were determined at the MP2(FC)/6-31G(d) level of theory and scaled by a factor of 0.9434.[21] Geometry optimizations for the larger ($n = 2-6$) sandwich complexes were done with the B3LYP/6-31G(d) density functional method. All calculations were performed using the GAUSSIAN98 computational package.[22]

3. Results and Discussion

The optimized structural parameters for $Li{\cdot}C_6H_6$ and $Li^+{\cdot}C_6H_6$ are presented in Table 1, and those for $Li{\cdot}(C_6H_6)_2$ and $Li^+{\cdot}(C_6H_6)_2$ are presented in Table 2. These structures were fully optimized at the MP2(FC)/6-31G(d) level of theory. The

TABLE 2: MP2(FC)/6-31G(d) Optimized Geometries of the Li·(C$_6$H$_6$)$_2$ and Li$^+$·(C$_6$H$_6$)$_2$ Complexes^a

parameter	Li·(C$_6$H$_6$)$_2$ (D_{2h})	Li·(C$_6$H$_6$)$_2$ (C_{2v})	Li$^+$·(C$_6$H$_6$)$_2$ (D_{6h})
r(C$_1$C$_1$)	1.393 (1.391)^b	1.385	1.404
r(C$_2$C$_2$)		1.400	
r(C$_1$C$_1'$)	1.422(1.422)	1.441	
r(C$_2$C$_2'$)		1.404	
r(C$_1$H$_1$)	1.088(1.087)	1.089	1.087
r(C$_2$H$_2$)		1.087	
r(C$_1$H$_1'$)	1.085(1.084)	1.085	
r(C$_2$H$_2'$)		1.086	
r(LiX$_1$)^a	1.769(1.872)	1.639	1.973
r(LiX$_2$)^a		1.999	
∠(C$_1$C$_1'$C$_1$)	118.3(118.6)	116.5	120.0
∠(C$_1'$C$_1$ C$_1$)	120.7(120.7)	121.0	
∠(C$_2$C$_2'$C$_2$)		119.7	
∠(C$_2'$C$_2$ C$_2$)		120.1	
d(C$_1$C$_1'$C$_1$ C$_1$)	6.1(4.0)	14.1	0.0
d(C$_2$C$_2'$C$_2$ C$_2$)		−1.4	

^{a} X$_1$ and X$_2$ refer to the centers of the two benzene rings. Bond and dihedral angles in degrees, and bond lengths in angstroms. (See Figure 1 for definition of labels.) ^{b} B3LYP/6-31G(d) results in parentheses.
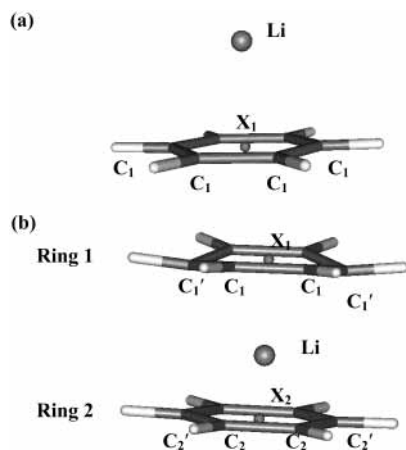

Figure 1. Structure and labels for the optimized (a) Li·(C$_6$H$_6$) and (b) Li·(C$_y$H$_6$)$_2$ D_{2h} and C_{2v} complexes. Structures were optimized at the MP2(FC)/6-31G(d) level of theory.

structures of Li·C$_6$H$_6$ and Li·(C$_6$H$_6$)$_2$ are illustrated in Figure 1. The dissociation energies ΔE_e for these neutral complexes are defined as

$$\Delta E_e = \{E[\text{Li}] + mE[\text{C}_6\text{H}_6]\} - \{E[\text{Li}(\text{C}_6\text{H}_6)_m]\}, \quad m = 1, 2 \tag{1}$$

where m is the number of benzene rings. The dissociation energies are defined similarly for the complexes with Li$^+$. The term ΔE_0 refers to dissociation energies (ΔE_e) with the addition of zero-point energy contributions. The dissociation energies at the HF/6-31G(d), B3LYP/6-31G(d), MP2(FC)/6-31G(d), MP2(FC)/G3MP2Large, QCISD(T)/6-31G(d), and G3(MP2) levels of theory are presented in Table 3.

3.1. Benzene Complexes with Li Atom. *Li·C$_6$H$_6$.* The Li·C$_6$H$_6$ complex has a C_{6v} structure, with the Li atom located 2.252 Å from the center of the benzene ring (see Figure 1, Table 1). The G3(MP2) dissociation energy, including the MP2(FC)/6-31G(d) zero-point energy contribution, is 0.20 eV (see Table 3). At the HF/6-31G(d) level of theory, the complex is only bound by 0.08 eV. The weak binding at HF/6-31G(d) is due to the neglect of electron correlation, since the MP2/6-31G(d) and QCISD(T)/6-31G(d) dissociation energies are much larger (0.33 and 0.32 eV, respectively).

Li·(C$_6$H$_6$)$_2$. MP2(FC)/6-31G(d) optimized geometries for D_{2h} and C_{2v} structures of Li·(C$_6$H$_6$)$_2$ are presented in Table 2. The D_{6h} structure distorts due to the Jahn−Teller effect.[23] The lowest unoccupied orbitals (LUMO) for Li$^+$·(C$_6$H$_6$)$_2$ are degenerate, having e$_{2g}$ symmetry. In the neutral Li·(C$_6$H$_6$)$_2$ complex, which has a single electron added to one of these degenerate orbitals, geometry relaxation results in a D_{2h} structure with the highest occupied molecular orbital (HOMO) having a$_g$ symmetry and is a ^{2}A$_g$ state. In this structure, both benzene rings distort from their planar geometry, "folding" on an axis between the C$_1'$ carbon atoms, with the fold away from the lithium atom (as shown in Figure 1). At the MP2(FC)/6-31G(d) level, the two C$_1'$ atoms are 3.1° out of the benzene plane, and lie 0.04 Å closer to the lithium atom than the four C$_1$ atoms. Both rings are 1.769 Å away from the central Li atom.

According to Jotham and Kettle,[24] a C_{2h} structure can also arise from the degenerate e$_{2g}$ mode, but we were unable to find a minimum with this symmetry; however, we did find a stable C_{2v} structure (see Table 2). Its highest occupied molecular orbital (HOMO) has a$_1$ symmetry and is a ^{2}A$_1$ state. This structure has the same "folding" distortions of the planar benzene rings as found in the D_{2h} structure; however, the distortion is markedly asymmetric in the C_{2v} case. At the MP2(FC)/6-31G(d) level, the two C$_1'$ atoms (ring 1) are 14.1° out of the benzene plane, and lie 0.10 Å closer to the lithium atom than the four C$_1$ atoms. The second benzene ring (ring 2) mirrors this distortion, but to a lesser extent. The C$_2'$ carbon atoms lie only 1.4° out of the benzene plane, and are only 0.01 Å closer to the lithium atom than the remaining carbon atoms. Ring 1 is also significantly closer than ring 2 to the central lithium atom (1.639 Å versus 1.999 Å).

The results in Table 3 indicate that correlation effects make significant contributions to the dissociation energy of Li·(C$_6$H$_6$)$_2$. At the HF/6-31G(d) level of theory, a minimum was not found for the D_{2h} complex, but a metastable state was found for the C_{2v} complex. This state is a minimum on the potential energy surface, but was predicted to be unbound by 0.26 eV, with respect to Li and two C$_6$H$_6$ molecules. The C_{2v} complex becomes bound when electron-correlation is included with the MP2/6-31G(d) method, increasing the dissociation energy (ΔE_e) by 0.91 eV to 0.65 eV. The D_{2h} complex is more stable with a dissociation energy of 0.85 eV (0.20 eV larger than the C_{2v} complex) at the MP2/6-31G(d) level of theory. The final G3(MP2) dissociation energy for the D_{2h} complex, with zero-point energy contributions, is 0.85 eV.

At the B3LYP/6-31G(d)//B3LYP/6-31G(d) level of theory, only a D_{2h} structure was found with a dissociation energy (ΔE_0) of 0.84 eV, in good agreement with the G3(MP2) result of 0.85 eV. The B3LYP/6-31G(d) geometry also agrees reasonably well with the MP2/6-31G(d) geometry (see Table 2), with the greatest deviation being the distance from the Li atom to the benzene rings, which is 1.872 Å at the B3LYP/6-31G(d) level, versus 1.769 Å at the MP2/6-31G(d) level.

We note that the MP2/6-31G(d) calculations for the two optimized Li·(C$_6$H$_6$)$_2$ structures are based on unstable Hartree−Fock (HF) wave functions. The HF wave function for the D_{2h} structure is unstable with respect to the reduced symmetry C_{2v} solution, and the HF wave function for the C_{2v} structure is unstable with respect to a highly spin contaminated state (expectation value of the S^2 operator is ∼1.2). The B3LYP/6-31G(d) method does not have these problems and predicts a D_{2h} structure similar to that predicted by the MP2 calculations.

3.2. Benzene Complexes with Li$^+$ Cation. *Li$^+$·C$_6$H$_6$.* At the MP2(FC)/6-31G(d) level the Li$^+$·C$_6$H$_6$ complex has a C_{6v}

Lithium−Benzene Sandwich Compounds

J. Phys. Chem. A, Vol. 106, No. 41, 2002 **9535**

TABLE 3: Dissociation Energies[a] (eV) of the Li·(C$_6$H$_6$)$_m$ and Li$^+$·(C$_6$H$_6$)$_m$ Complexes (m = 1, 2)

method	dissociation energy type[a]	Li·C$_6$H$_6$ (C_{6v})	Li·(C$_6$H$_6$)$_2$ (D_{2h})	Li·(C$_6$H$_6$)$_2$ (C_{2v})	Li$^+$·C$_6$H$_6$ (C_{6v})	Li$^+$·(C$_6$H$_6$)$_2$ (D_{6h})
HF/6-31G(d)//HF/6-31G(d)	ΔE_e	0.08	b	−0.26	1.76	2.90
MP2/6-31G(d)//MP2/6-31G(d)	ΔE_e	0.33	0.85	0.65	1.90	3.52
MP2/G3MP2Large//MP2/6-31G(d)	ΔE_e	0.19	1.09		1.62	2.94
QCISD(T)/6-31G(d)//MP2/6-31G(d)	ΔE_e	0.32	0.67		1.87	3.40
B3LYP/6-31G(d)//B3LYP/6-31G(d)	ΔE_e	0.15	0.74	c	1.84	3.02
B3LYP/6-31G(d)//B3LYP/6-31G(d)	ΔE_0	0.20	0.84		1.82	3.03
G3(MP2)	ΔE_e	0.25	0.97		1.58	2.82
G3(MP2)	ΔE_0	0.20	0.85^b		1.49	2.67

^{a} See eq 1 for the definition of dissociation energy. Zero-point energy contributions are included in the ΔE_0 results, while the ΔE_e results do not include zero-point contributions. ^{b} For the D_{2h} structure the Hartree−Fock wave function was unstable, so it was not possible to find a stable HF/6-31G(d) minimum, and the MP2/6-31G(d)//MP2/6-31G(d) frequency also had an unrealistically large frequency due to this wave function instability. Instead, the MP2/6-31G(d)//MP2/6-31G(d) C_{2v} zero-point contributions were used to estimate ΔE_0. ^{c} Collapses to D_{2h} structure.

TABLE 4: Mulliken and Natural Bond Order (NBO) Charges and Populations for the Li·(C$_6$H$_6$)$_m$ and Li$^+$·(C$_6$H$_6$)$_m$ Complexes (m = 1, 2), at the HF/6-31G(d)//MP2(FC)/6-31G(d) Level of Theory[a]

	Li·C$_6$H$_6$		Li·(C$_6$H$_6$)$_2$ (D_{2h})		Li·(C$_6$H$_6$)$_2$ (C_{2v})		Li$^+$·(C$_6$H$_6$)		Li$^+$·(C$_6$H$_6$)$_2$	
charges	Mulliken	NBO	Mulliken	NBO	Mulliken	NBO	Mulliken	NBO	Mulliken	NBO
Li	−0.215	−0.005	0.105 (0.994)^a	0.917	0.141 (0.969)^a	0.917	0.493	0.961	0.187	0.923
ring 1	0.215	0.005	−0.052 (−0.497)	−0.459	−0.374 (−0.935)	−0.917	0.507	0.039	0.407	0.039
ring 2			−0.052 (−0.497)	−0.459	0.233 (−0.034)	0.0			0.407	0.039
populations										
Li 2s	0.065	0.939	0.128	0.067	0.115	0.065	0.093	0.014	0.084	0.056
Li 2p$_x$	0.047	0.004	0.184	0.002	0.145	0.006	0.127	0.000	0.159	0.001
Li 2p$_y$	0.047	0.004	0.170	0.004	0.181	0.007	0.127	0.000	0.159	0.001
Li 2p$_z$	0.177	0.055	0.150	0.004	0.168	0.002	0.082	0.000	0.173	0.001

^{a} Values in parentheses are the HF/G3MP2Large//MP2/6-31G(d) results.

structure, with the Li$^+$ lying 1.921 Å above the center of the benzene plane (see Table 1). The C−C bond lengths of the complex are slightly longer (0.004 Å) than those in the isolated benzene, which is consistent with some of the electron density being donated from the benzene ring to the Li$^+$. Our results are consistent with previous theoretical studies[3,5,6,8] on this complex. The G3(MP2) dissociation energy is 1.49 eV, including zero-point energies. This prediction is in good agreement with the previous experimental results of 1.58 ± 0.08[1,3] and 1.67 ± 0.14 eV.[3]

Li$^+$·(C$_6$H$_6$)$_2$. The Li$^+$·(C$_6$H$_6$)$_2$ complex has a D_{6h} structure, with C−C and C−H bond lengths similar to those in Li$^+$·C$_6$H$_6$ (see Table 2). The MP2(FC)/6-31G(d) distance of Li$^+$ from the center of the benzene rings is 1.973 Å, which is 0.052 Å longer than in Li$^+$·C$_6$H$_6$. The Li$^+$·(C$_6$H$_6$)$_2$ complex does not have a Jahn−Teller distortion. Previous MP2(full)/6-31G(d) and MP2-(full)/6-311+G(d) optimized geometries[3] for Li$^+$·(C$_6$H$_6$)$_2$ had slightly shorter distances of Li$^+$ from the center of the benzene rings, with bond lengths of 1.950 and 1.917 Å, respectively. Our final G3(MP2) dissociation energy, with zero-point energies, of 2.67 eV compares well to the experimental value[3] of 2.75 ± 0.21 eV.

3.3. Comparison of Li·(C$_6$H$_6$)$_2$ with Li·C$_6$H$_6$, Li$^+$·C$_6$H$_6$, and Li$^+$·(C$_6$H$_6$)$_2$ Complexes. The dissociation energies presented in the previous section indicate a surprising stability for the Li·(C$_6$H$_6$)$_2$ complex. The dissociation energies of Li$^+$·C$_6$H$_6$ and Li$^+$·(C$_6$H$_6$)$_2$ of 1.49 and 2.67 eV, respectively, are consistent with a primarily electrostatic interaction between the Li$^+$ and the ligands, while the dissociation energy of Li·C$_6$H$_6$ of 0.20 eV is consistent with a dispersion interaction. The dissociation energies for the Li·(C$_6$H$_6$)$_2$ complex is about four times that of Li·(C$_6$H$_6$) and cannot be attributed solely to dispersion.

An explanation for the surprising stability of the Li·(C$_6$H$_6$)$_2$ complex is provided by a Natural Bond Order (NBO)[25] population analysis. These NBO populations and charges are presented in Table 4. At the HF/6-31G(d)//MP2/6-31G(d) level,

the NBO method gives a positive charge of 0.92 on the Li atom, in the sandwich complex, with the negative charge evenly distributed over both rings (−0.459 per ring). [In the C_{2v} case, all of the negative charge is transferred to only one of the benzene rings (ring1 in Figure 1).] Thus, the D_{2h} Li·(C$_6$H$_6$)$_2$ complex appears to exhibit charge separation corresponding to C$_6$H$_6^{-1/2}$−Li$^+$−C$_6$H$_6^{-1/2}$. This charge separation explains the unusually strong dissociation energy found for Li·(C$_6$H$_6$)$_2$. It also explains the short Li−benzene distances of 1.769 Å found for the complex, which is significantly less than the Li$^+$−benzene distance of 1.973 Å in Li$^+$·(C$_6$H$_6$)$_2$.

Calculation of Mulliken[26] charges in the Li·(C$_6$H$_6$)$_2$ complexes indicates a case of dramatic failure of the Mulliken population analysis. In contrast to the NBO results the Mulliken analysis gives a positive charge of only 0.10 on Li in the D_{2h} structures, at the HF/6-31G(d) level (see Table 4); however, use of the larger G3MP2Large basis set dramatically increases the Mulliken charge on Li to 0.994, more consistent with the NBO charges. This sensitivity of Mulliken populations to the basis set has been noted previously.[25] The HF/6-31G(d) Mulliken charges on lithium in the cation complexes [Li$^+$·C$_6$H$_6$ and Li$^+$·(C$_6$H$_6$)$_2$] are also much smaller than the NBO charges (see Table 4).

3.4. Discussion of Bonding Trends in Larger Sandwich Complexes, Li$_n$·(C$_6$H$_6$)$_{n+1}$, n = 2−6. The unexpectedly large dissociation energy found for the Li·(C$_6$H$_6$)$_2$ complexes raises the question of whether the strong binding in this system extends to larger Li$_n$·(C$_6$H$_6$)$_{n+1}$ complexes. To answer this question we optimized the structures for Li$_n$·(C$_6$H$_6$)$_{n+1}$ complexes, for n = 1−6. For computational efficacy we constrained the geometries to the D_{6h} point group, and used the density functional B3LYP/6-31G(d) method. In these optimizations we forced all Li-X distances in the complex to be equal. We tested this constraint by removing it and reoptimizing the geometry of Li$_3$·(C$_6$H$_6$)$_4$. The reoptimized geometry had a dissociation energy within 0.0002 eV of that found for the constrained structure, and nearly
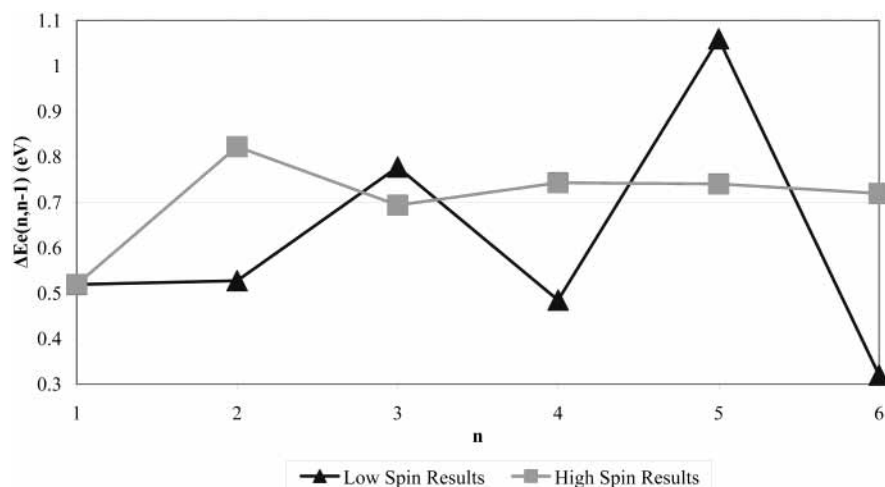
Figure 2. Plot of the energy required to dissociate a single $Li \cdot C_6H_6$ unit from the $Li_n \cdot (C_6H_6)_{n+1}$ complex versus the number of Li atoms in the complex.

TABLE 5: B3LYP/6-31G(d) Geometries and Dissociation Energies (eV) for $Li_n(C_6H_6)_{n+1}$ Complexes ($n = 1-6$)

complex	multiplicity	$r(LiX)$ (Å)	$\Delta E_e{}^a$	$\Delta E_e(n,n-1)^a$
$Li \cdot (C_6H_6)_2$	2	1.901	0.67	0.52
$Li_2(C_6H_6)_3$	1	1.852	1.35	0.53
$Li_2(C_6H_6)_3$	3	1.852	1.64	0.82
$Li_3(C_6H_6)_4$	2	1.838	2.27	0.78
$Li_3(C_6H_6)_4$	4	1.865	2.49	0.69
$Li_4(C_6H_6)_5$	1	1.822	2.91	0.48
$Li_4(C_6H_6)_5$	5	1.854	3.38	0.74
$Li_5(C_6H_6)_6$	2	1.851	4.12	1.06
$Li_5(C_6H_6)_6$	6	1.860	4.27	0.74
$Li_6(C_6H_6)_7$	1	1.826	4.59	0.32
$Li_6(C_6H_6)_7$	7	1.854	5.14	0.72

^{a} See eq 2 for the definition of ΔE_e, and see eq 3 for the definition of $\Delta E_e(n,n-1)$.

the same Li−X distances. Thus, this constraint seems to have minimal effect on the final dissociation energies for the complexes for $n \geq 2$. Due to the unpaired spin on the lithium atoms, the complexes with multiple lithium atoms can have several different spin states. We examined the effects of these different states by performing geometry optimizations for both the lowest and highest spin states for all complexes. In all cases the high spin states were found to be slightly more stable than the corresponding low spin predictions. This is consistent with the large separation (and consequently the weak interactions) between the lithium atoms; therefore the high spin states are favored in accordance with Hund's rule.

The geometries and dissociation energies for all of these complexes are in Table 5. The dissociation energy is defined as

$$\Delta E_e(n) = \{nE[Li] + (n+1)E[C_6H_6]\} - \{E[Li_n \cdot (C_6H_6)_{n+1}]\}, \quad n = 1-6 \quad (2)$$

The energy gain $\Delta E_e(n,n-1)$, with addition of a $Li \cdot C_6H_6$ unit to $Li_{n-1} \cdot (C_6H_6)_n$, is given by

$$\Delta E_e(n,n-1) = \{E[Li \cdot C_6H_6] + E[Li_{n-1} \cdot (C_6H_6)_n]\} - \{E[Li_n \cdot (C_6H_6)_{n+1}]\}, \quad n = 1-6 \quad (3)$$

In Figure 2 we plot $\Delta E_e(n,n-1)$ versus the number of Li atoms in the complex. For the high spin case, $\Delta E_e(1,0)$ is 0.52 eV and $\Delta E_e(2,1)$ is 0.82 eV, an increase of 0.3 eV. This indicates a cooperative interaction that favors the double-decker sandwich

complex, $n = 2$. The energy gain for adding subsequent $Li \cdot C_6H_6$ units levels off around 0.74 eV at $n = 4$.

The total dissociation energies $\Delta E_e(n)$ of the high-spin complexes converge to about 0.85 eV/Li atom. The low-spin states oscillate somewhat, because the doublet states consistently have slightly higher dissociation energies/Li atom $[\Delta E_e(n)/n]$ than the singlet states, converging to ∼0.75 eV/Li atom. Thus, the stability found in the $Li \cdot (C_6H_6)_2$ complexes extends to larger $Li_n \cdot (C_6H_6)_{n+1}$ complexes.

Although we have found no previous experimental or theoretical studies on multidecker alkali metal−benzene complexes, there has been some work on multidecker transition metal−benzene complexes.[11,14] Specifically, dissociation energies were predicted with density functional theory for $V \cdot (C_6H_6)_2$, $V_2 \cdot (C_6H_6)_3$, $Fe \cdot (C_6H_6)_2$, and $Fe_2 \cdot (C_6H_6)_3$. These results differ from our $Li \cdot (C_6H_6)_2$ and $Li_2 \cdot (C_6H_6)_3$ results in two regards. First, Pandey et al.[14] found singlet configurations to be more favorable than the triplet states for the $V_2 \cdot (C_6H_6)_3$ and $Fe_2 \cdot (C_6H_6)_3$ complexes, whereas we found the triplet state to be more favorable for $Li_2 \cdot (C_6H_6)_3$. They also found $\Delta E_e(2,1)$ to be significantly smaller than $\Delta E_e(1,0)$ for both V and Fe, whereas we found the opposite to be true for the Li complexes. Specifically, $\Delta E_e(n,n-1)$ increases by 0.3 eV from $Li \cdot (C_6H_6)_2$ to $Li_2 \cdot (C_6H_6)_3$, while $\Delta E_e(n,n-1)$ decreases by 2.14 eV from $V \cdot (C_6H_6)_2$ to $V_2 \cdot (C_6H_6)_3$, and by 0.54 eV from $Fe \cdot (C_6H_6)_2$ to $Fe_2 \cdot (C_6H_6)_3$. The findings for the V and Fe complexes are consistent with mass spectra,[11] where peak intensities were smaller for complexes larger than $M \cdot (C_6H_6)_2$. For the Li multidecker complexes, the fact that $\Delta E_e(n,n-1)$ increases before remaining nearly constant (after a slight decrease at $n = 3$) suggests that larger multidecker complexes may exist for this system. Preliminary calculations were also performed for the $Na \cdot (C_6H_6)_2$ and $K \cdot (C_6H_6)_2$ complexes, at the B3LYP/6-31G(d) level of theory. Stable D_{2h} structures were found for both complexes; however, the weak dissociation energies (less than 0.1 eV) minimize the likelihood of isolating these complexes experimentally.

4. Conclusions

We have used quantum chemical methods to examine the bonding in lithium-benzene sandwich compounds. The neutral $Li \cdot (C_6H_6)_2$ complex had a surprisingly large dissociation energy ΔE_0 of 0.85 eV, at the G3(MP2) level of theory, and 0.84 eV, at the B3LYP/6-31G(d) level. Short benzene−benzene distances

Lithium−Benzene Sandwich Compounds

J. Phys. Chem. A, Vol. 106, No. 41, 2002 **9537**

of 3.546 and 3.744 Å were found at the MP2(FC)/6-31G(d) and B3LYP/6-31G(d) levels, respectively, which are shorter than in $Li^{+} \cdot (C_6H_6)_2$. The increased binding is due to the formation of a charge-separated species, $C_6H_6^{-1/2}-Li^{+}-C_6H_6^{-1/2}$, having fairly strong electrostatic interactions. We have extended these calculations out to $Li_6 \cdot (C_6H_6)_7$, by adding subsequent $Li \cdot C_6H_6$ units. All of these compounds demonstrated strong binding between the Li atom and the benzene rings, and converged to a dissociation energy of approximately 0.85 eV/Li atom, for the high spin states, at the B3LYP/6-31G(d) level of theory.

References and Notes

(1) Woodin, R. L.; Beauchamp, J. L. *J. Am. Chem. Soc*. **1978**, *100*, 501.

(2) Taft, R. W.; Anvia, F.; Gal, J.-F.; Walsh, S.; Capon, M.; Holmes, M. C.; Hosn, K.; Oloumia, G.; Vasanwala, R.; Yazdani, S. *Pure Appl. Chem.* **1990**, *62*, 17.

(3) Amicangelo, J. C.; Armentrout, P. B. *J. Phys. Chem. A* **2000**, *104*, 11420.

(4) Hoyau, S.; Norrman, K.; McMahon, T. B.; Ohanessian, G. *J. Am. Chem. Soc.* **1999**, *121,* 8864.

(5) Nicholas, J. B.; Hay, B. P.; Dixon, D. A. *J. Phys. Chem. A* **1999**, *103*, 1394.

(6) Feeler, D.; Dixon, D. A.; Nicholas, J. B. *J. Phys. Chem. A* **2000**, *104*, 11414.

(7) Tsuzuki, S.; Yoshida, M.; Uchimaru, T.; Mikami, M. *J. Phys. Chem. A* **2001**, *105*, 769.

(8) Caldwell, J. W.; Kollman, P. A. *J. Am. Chem. Soc.* **1995**, *117*, 4177.

(9) Zhengyu, Z.; Jian, X.; Chuanson, Z.; Xingming, Z.; Dongmei, D.; Kezhong, Z. *Theochem.* **1999**, *469*, 1.

(10) Hoshino, K.; Kurikawa, T.; Takeda, H.; Nakajima, A.; Kaya, K. *J. Phys. Chem.* **1995**, *99*, 3053.

(11) Kurikawa, T.; Takeda, H.; Nakajima, A.; Kaya, K. *Z. Phys. D* **1997**, *40,* 65.

(12) Yasuike, T.; Yabushita, S. *J. Phys. Chem. A* **1999**, *103*, 4533.

(13) Nakajima, A.; Kaya, K. *J. Phys. Chem. A* **2000**, *104*, 176.

(14) Pandey, R.; Rao, B. K.; Jena, P.; Blanco, M. A. *J. Am. Chem. Soc.* **2001**, *123*, 3799.

(15) Sahnoun, R.; Mijoule,C. *J. Phys. Chem. A* **2001**, *105*, 6176.

(16) Hong, G.; Schautz, F.; Dolg, M. *J. Am. Chem. Soc.* **1999**, *121*, 1502.

(17) Hehre, W. J.; Radom, L.; Schleyer, P. v. R.; Pople, J. A. *Ab Initio Molecular Orbital Theory*; John Wiley and Sons: New York, 1986.

(18) Becke, A. D. *J. Chem. Phys.* **1993**, *98*, 5648.

(19) Stephens, P. J.; Devlin, F. J.; Chabalowski, C. F.; Frisch, M. J. *J. Phys. Chem.* **1994**, *98*, 11623.

(20) Curtiss, L. A.; Redfern, P. C.; Raghavachari, K.; Rassolov, V.; Pople, J. A. *J. Chem. Phys.* **1999**, *110*, 4703.

(21) Scott, A. P.; Radom, L. *J. Phys. Chem.* **1996**, *100*, 16502.

(22) Frisch, M. J.; Trucks, G. W.; Schlegel, H. B.; Scuseria, G. E.; Robb, M. A.; Cheeseman, J. R.; Zakrzewski, V. G.; Montgomery, Jr., J. A.; Stratmann, R. E.; Burant, J. C.; Dapprich, S.; Millam, J. M.; Daniels, A. D.; Kudin, K. N.; Strain, M. C.; Farkas, O.; Tomasi, J.; Barone, V.; Cossi, M.; Cammi, R.; Mennucci, B.; Pomelli, C.; Adamo, C.; Clifford, S.; Ochterski, J.; Petersson, G. A.; Ayala, P. Y.; Cui, Q.; Morokuma, K.; Malick, D. K.; Rabuck, A. D.; Raghavachari, K.; Foresman, J. B.; Cioslowski, J.; Ortiz, J. V.; Baboul, A. G.; Stefanov, B. B.; Liu, G.; Liashenko, A.; Piskorz, P.; Komaromi, I.; Gomperts, R.; Martin, R. L.; Fox, D. J.; Keith, T.; Al-Laham, M. A.; Peng, C. Y.; Nanayakkara, A.; Gonzalez, C.; Challacombe, M.; Gill, P. M. W.; Johnson, B. G.; Chen, W.; Wong, M. W.; Andres, J. L.; Head-Gordon, M.; Replogle, E. S.; Pople, J. A. *Gaussian 98*, revision A.7; Gaussian, Inc.: Pittsburgh, PA, 1998.

(23) Jahn, H. A.; Teller, E. *Proc. R. Soc.* **1937**, *A161*, 220.

(24) Jotham, R. W.; Kettle, S. F. A.; *Inorgan. Chim. Acta*, **1971**, *5*, 183.

(25) Reed, A. E.; Curtiss, L. A.; Weinhold, F. *Chem. Rev.* **1988**, *88*, 899.

(26) Mulliken, R. S. *J. Chem. Phys.* **1955**, *23*, 1833.